Enhancing the waveguide-resonator optical force with an all-optical on-chip analog of electromagnetically induced transparency

Varat Intaraprasonk
Department of Applied Physics, Stanford University, Stanford, California 94305, USA

Shanhui Fan
Department of Electrical Engineering, Stanford University, Stanford, California 94305, USA

(Received 19 August 2012; published 26 December 2012)

We demonstrate a fundamental limitation in the force enhancement in simple waveguide-resonator geometry. We also show that the all-optical analog to electromagnetically induced transparency, as observed in a waveguide-resonator geometry, can be used to drastically enhance waveguide-resonator optical force, significantly beyond what one can achieve in principle in conventional waveguide-resonator coupling schemes.

DOI: 10.1103/PhysRevA.86.063833 PACS number(s): 42.60.Da, 42.50.Gy, 42.82.−m

Pursuing an all-optical on-chip analog of electromagnetically induced transparency (EIT) [1] has been of fundamental interest [2–10] because it highlights the conceptual link between optical microresonator physics and atomic physics [7]. Novel applications include slow and stopped light, which is achieved by a very flat band structure due to the dark state's small external coupling [8,9]. Another example of the applications is for sensing, which utilizes the system's high sensitivity to the change in the index of refraction of its environment [10]. The EIT effect was also recently incorporated with the fields of plasmonics and metamaterials since this effect can be used to reduce external radiation and hence enhance the quality factor of the resonance [11,12].

In this paper, we consider a waveguide-resonator geometry consisting of two waveguides coupled through two ring resonators in between [Fig. 1(a)]. Experimentally, it has been shown that this geometry exhibits a pronounced EIT-like transmission spectrum [3]. Here we show that the same all-optical EIT effect can be exploited to greatly enhance optical force. We will show that this scheme can achieve the force far more than is obtainable, in principle, in the traditional waveguide-resonator configuration consisting of a single resonator [Fig. 1(b)].

The use of an optical ring resonator to enhance optical force has been explored very extensively [13–20]. Among all the geometries explored, the waveguide-ring configuration, as shown in Fig. 1(b), was of interest because of its application in actuation, filtering, and optomechanical cooling [13–15]. In general, in using an optical resonator to enhance optical force, one uses a high quality-factor (Q-factor) cavity such that the field generated by each incident photon is enhanced, which then translates into a higher optical force per incident photon. In the waveguide-ring geometry, one would like similarly to use the high-Q cavity to enhance the waveguide-cavity force. However, in this system, the external Q factor that describes the waveguide-cavity coupling can only be increased by increasing the distance between the waveguide and the cavity. Such an increase, unfortunately, also reduces the force per photon in the cavity. As a result, the capability of the resonator force enhancement in this geometry is limited.

The origin of the optical force can be explained as the gradient of the energy landscape of the resonating photon energy and output power, with respect to relevant physical displacements [13,21,22]. As a concrete example, we study the waveguide-ring configuration as shown in Fig. 1(b). The system is chosen to be in two dimensions with electric field strictly along the z direction. We are interested in the system with the resonance near the telecommunication free-space wavelength of 1550 nm; therefore, in this paper, we normalize all quantities with respect to a length scale of $a = 1\ \mu$m so they are on the order of unity. The resonator is racetrack-shaped. Both the resonator track and the waveguide are $0.2a$-wide-slabs of silicon with dielectric constant $\epsilon_{\mathrm{Si}} = 12.1$. They are separated by an edge-to-edge distance d and surrounded by air with $\epsilon_{\mathrm{air}} = 1$. The resonator track has curved sections with a radius of $r = 1\ \mu$m, and straight sections of length L. At $L = 0$, the resonance frequency is approximately $0.64c/a$, where c is the speed of light in vacuum. Because the effective wavelength of the fundamental mode of a silicon waveguide with the same width of $0.2a$ is $\lambda_w = 0.57a$ nm at this frequency, L will be chosen as a multiple of $\lambda_w/2$ to maintain roughly the same resonance frequency. The optical force between the resonator and the waveguide is calculated by integrating the Maxwell stress tensor in a finite-element frequency-domain simulation package, COMSOL [23].

Since we consider a two-dimensional (2D) system, the total force, as determined by a line integral of the stress tensor, is in units of N/m, and the power is in units of W/m. Since the force is proportional to the input power, we will present the force in the normalized unit of $(\mathrm{N/m})/(\mathrm{W/m}) = \mathrm{N/W}$. Also, we will make a comparison between the waveguide-cavity force and the force between parallel waveguides [Fig. 1(d)]. The correct measure of the waveguide-waveguide force is the 2D force per unit length along the waveguide direction, which has the unit of $(\mathrm{N/m})/\mathrm{m} = \mathrm{N/m^2}$. Thus, the 2D waveguide-waveguide force is the pressure. Again normalizing with respect to the input power in two dimensions, the pressure will be presented in the unit of $(\mathrm{N/m^2})/(\mathrm{W/m}) = \mathrm{N/(W\,m)}$. Knowing the typical value of the pressure in the waveguide-cavity configuration, the waveguide-cavity force can be simply estimated by multiplying the pressure with the effective coupling length along the waveguide direction, which is roughly the radius r in this configuration. Note that even though our setup is in two dimensions, the value of the optical pressure calculated

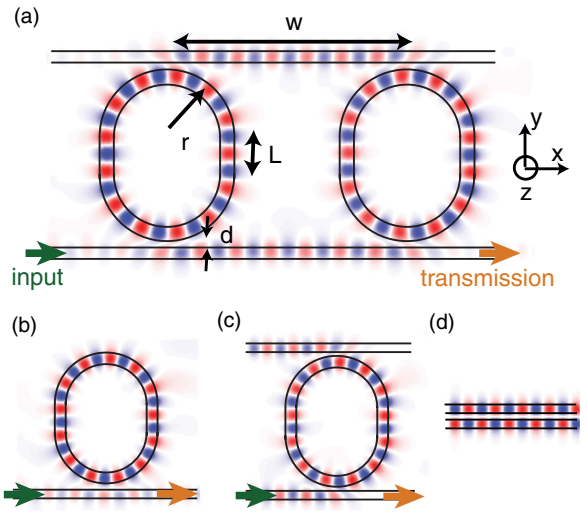

FIG. 1. (Color online) Diagrams of various waveguide-resonator setups. (a) EIT setup, (b) conventional waveguide-cavity setup, (c) two-waveguide–single-resonator setup, (d) parallel waveguides setup. Blue and red color mapping shows the magnitude of the electric field (positive and negative values). The frequency for each plot is chosen near the resonance near $0.64c/a$. Green and orange arrows denote input and output (transmission) ports, respectively.

here should be approximately equal to those obtained in three-dimensional experiments or simulations, where the cross sections of the resonator and the waveguide are rectangular. This is because both the pressure and the power should have similar z dependence, so this dependence should cancel out in the calculation of pressure-power ratio. Therefore, the enhancement effect that we observe in two dimensions should be achievable in 3D structures as well.

For the structure shown in Fig. 1(b), we plot in Fig. 2(a) the maximum waveguide-resonator pressure (F_{wr}) as a function

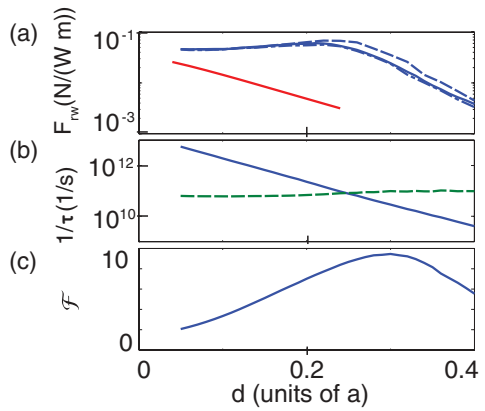

FIG. 2. (Color online) Calculated results for configuration in Fig. 1(b) as a function of the distance d between either waveguide-resonator or waveguide-waveguide. (The waveguides have a radius $r = a = 1\ \mu$m, a width of $0.2a$, $\epsilon_{\mathrm{Si}} = 12.1$, surrounded by air, $\epsilon_{\mathrm{air}} = 1$. The resonator has resonance near $0.64c/a$.) (a) Pressures: waveguide-resonator pressure F_{wr} for $L = \lambda_w, 4\lambda_w, 7\lambda_w$ (solid, dashed, dash-dotted lines, respectively) and waveguide-waveguide pressure F_{ww} (dotted line). (b) Waveguide-resonator coupling rates: $1/\tau_e$ (solid) and $1/\tau_0$ (dashed). (c) Resonator field enhancement $\mathcal{F}$.

of waveguide-cavity spacing d for a few structures with a different straight section length L, chosen such that the resonance is fixed around $0.64c/a$. We then consider the frequencies in the vicinity of that resonance. The data points in Fig. 2(a) correspond to the maximum repulsive pressure among all frequencies around the resonance, and all spatial regions along the waveguide. We find that the optical pressure is bipolar as the frequency varies across the resonance [15], with the repulsive pressure being dominant for our setup. The pressure reaches a plateau at small d ($d \lesssim 0.2a$) and decays exponentially at larger d.

To quantify the pressure enhancement due to the resonator, it is useful to find a "base" case to compare the pressure to. From the plot of the field in Fig. 2(a), we can see that the resonator field profile looks similar to the field in the waveguide, as expected from such a ring resonator. Therefore, a natural choice of the base case is the pressure between two parallel waveguides of the same width and the same spacing d [Fig. 1(d)]. To compare with dominantly repulsive pressure in the resonator setup, we choose the odd-mode excitation for the waveguide-waveguide case in order to generate a repulsive pressure [22,24]. This pressure F_{ww} between the two parallel waveguides thus determined exhibits an exponential decay as a function of d, as shown in Fig. 2(a). We can see that F_{wr} is, as expected, higher than F_{ww}. The pressure enhancement, however, is quite small; the maximum of F_{wr} is only twice F_{ww} at $d = 0.05a$.

This behavior of the optical pressure as a function of d can be explained with the coupled mode theory [25]. In that theory, the key parameters are the external coupling rate or external linewidth ($1/\tau_e$), and the intrinsic loss rate or intrinsic linewidth ($1/\tau_0$). The external coupling rate is the exchange rate of the energy between the resonance and the waveguide. The intrinsic loss rate is the rate at which the cavity loses energy from other means, for example by radiation or material loss. These rates are directly calculated in the simulations by fitting the transmission and are plotted in Fig. 2(b). For $d < 0.25a$, $1/\tau_e > 1/\tau_0$, the system is in the overcoupling regime. For $d > 0.25a$, $1/\tau_e < 1/\tau_0$, the system is in the undercoupling regime. Comparing this to the pressure plot in Fig. 2(a), we can see that in the overcoupling regime the pressure reaches a plateau and is almost independent of d, while in the undercoupling regime the pressure decays exponentially as a function of d.

As a simple quantitative model, the waveguide-cavity pressure can be considered as the waveguide-waveguide pressure amplified by the field-enhancement factor ($\mathcal{F}$) of the resonator, defined as the ratio between the field inside the resonator and the input field,

$$F_{\mathrm{wr}}(d) \sim F_{\mathrm{ww}}(d)\mathcal{F}(d). \tag{1}$$

The waveguide-waveguide pressure decays exponentially with respect to d as seen in Fig. 2(a), i.e., $F_{\mathrm{ww}} \propto \exp(-k_d d)$, where k_d describes the evanescent decay of the field away from the waveguide. The field-enhancement factor near resonance, as plotted in Fig. 2(c), is given by

$$\mathcal{F} = \frac{\sqrt{\frac{2}{\tau_e T}}}{1/\tau_e + 1/\tau_0}, \tag{2}$$

where T is the round-trip time of the resonator. Thus the enhancement factor in general depends on both the internal and external linewidth. Because $1/\tau_e$ and $1/\tau_0$ depend on T, we factor out T by defining the dimensionless coupling constants $\kappa_e = (2T/\tau_e)^{1/2}$ and $\kappa_0 = (2T/\tau_0)^{1/2}$. This gives

$$\mathcal{F} = \frac{2\kappa_e}{\kappa_e^2 + \kappa_0^2}. \tag{3}$$

The dimensionless waveguide-cavity coupling constant κ_e decays exponentially with d, while κ_0 is approximately constant in d. Therefore, in the overcoupling regime ($\kappa_e \gg \kappa_0$), $\mathcal{F} \propto \exp(k_d d)$, the exponential dependency of which cancels out the decay of $F_{\rm ww}$ and gives a plateau in waveguide-cavity pressure. On the other hand, in the undercoupling regime ($\kappa_e \ll \kappa_0$), $\mathcal{F} \propto \exp(-k_d d)$, which results in a fast exponential decay of the waveguide-cavity pressure $F_{\rm wr}(d) \propto \exp(-2k_d d)$. This simple theory agrees well with the numerical results in Figs. 2(a) and 2(c).

As an additional confirmation of the theory, because the round-trip time T totally cancels out in Eq. (3), the pressure does not depend on the resonator size if the geometry of the coupling region is the same. This is confirmed in Fig. 2(a), where pressures are the same for different L's. As a side note, Ref. [13] shows an increase of optical pressure when the modal size of the resonator is reduced. However, in Ref. [13], the modal size is reduced by reducing r, which reduces the length of the coupling region. Our results here are not in conflict with those of Ref. [13].

To summarize the discussions above on the waveguide-cavity pressure in the single ring cavity configuration, we have shown that the pressure reaches a plateau in the overcoupling regime, and that the overall pressure enhancement, as compared to the waveguide-waveguide pressure, is rather limited, due to the opposite and canceling exponential dependency on d of the cavity field enhancement and the base pressure. While the waveguide-resonator geometry has been previously considered, the existence of such a limitation for pressure enhancement and its physical explanation have not been recognized before. Our theory implies that (i) increasing external Q, by increasing the cavity waveguide spacing, certainly does not enhance the optical pressure, and (ii) perhaps somewhat counterintuitively, making a resonator with lower loss (higher $1/\tau_0$) also cannot improve the pressure because the maximum pressure is achieved in the overcoupling regime, where $1/\tau_e$ dominates anyway. As a result, the overall pressure enhancement over the waveguide-waveguide pressure is rather limited.

Based on the above-mentioned analysis, we see that, to further enhance the waveguide-resonator optical pressure, it is important to decouple the field enhancement of the optical resonance, from the resonator-waveguide distance. We therefore consider the setup as shown in Fig. 1(a), consisting of two waveguides and two cavities. It is well known that this setup provides an all-optical analog to EIT. Here, we show that such an EIT analog provides a mechanism to drastically enhance the waveguide-resonator optical pressure.

The EIT analog in the setup of Fig. 1(a) arises from the resonant interference between the two resonators. To briefly review the underlying physics of the EIT analog, we consider first a structure consisting of a single ring resonator coupled to two waveguides [Fig. 1(c)]. For light incident from one of the waveguides, the transmission spectrum for the light power exiting the same waveguide [bottom right port in Fig. 1(c)] is shown in Fig. 3(a). The transmission spectrum exhibits a single Lorentzian dip, indicating typical single resonance behavior.

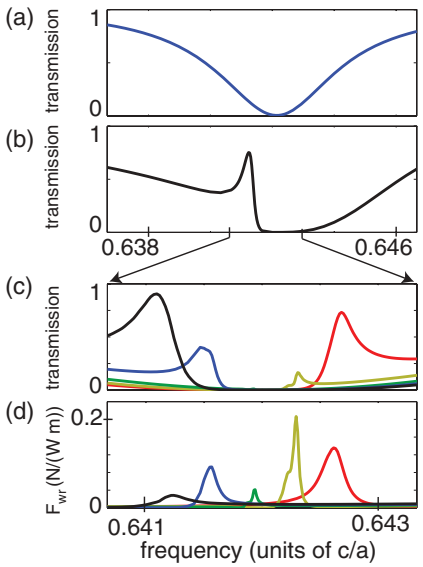

FIG. 3. (Color online) (a) Transmission as a function of frequency, for the two-waveguide-single-resonator setup with $L = \lambda_w$, $d = 0.1a$. (b) Transmission for the two-resonator-two-waveguide setup with $w = 4.03a$ (solid). (c) T and (d) $F_{\rm wr}$ as a function of frequency for the two-resonator setup with the same L and d for $w = 3.95a$ (red), $3.97a$ (yellow), $3.99a$ (green), $4.01a$ (blue), and $4.03a$ (black).

In the presence of the second cavity in the structure of Fig. 1(a), and with an appropriate choice of the cavity-cavity distance, the transmission spectra [bottom right port in Fig. 1(a)] now exhibit a pronounced "transparency resonance" peak within the resonance dip of a single cavity, as we can seen in Fig. 3(b). In Fig. 3(c), which is a more detailed view, we plot the transmission spectrum for a system with $L = \lambda_w$ and $d = 0.1a$ for five values of distances w between the two resonators. Such a transparency resonance is a direct optical analog to EIT; it arises due to the coherent destructive interference of the decaying amplitudes of the two resonances to the waveguides [3]. The linewidth of such a transparency resonance can be much smaller as compared to the linewidth of an individual resonator. Moreover, the linewidth can be controlled by changing w, as seen in Fig. 3(c). Therefore, the use of the EIT analog provides us with a mechanism to decouple the external resonator linewidth and the waveguide-resonator distance, allowing further field enhancement while keeping d constant. The EIT effect is therefore ideal for the enhancement of waveguide-resonator optical pressure.

To show that the EIT effect can indeed enhance the waveguide-cavity pressure, we calculate the waveguide-resonator pressure ($F_{\rm wr}$), which is defined to be the pressure on the input waveguide near the resonator closest to the input port. [The pressure between other pairs of resonator and waveguide should behave similarly, as can be seen from the field pattern in Fig. 1(a).] The result is plotted in Fig. 3(d) for five values of w. As can be seen, the pressure has sharp peaks at approximately the same frequency as the transmission

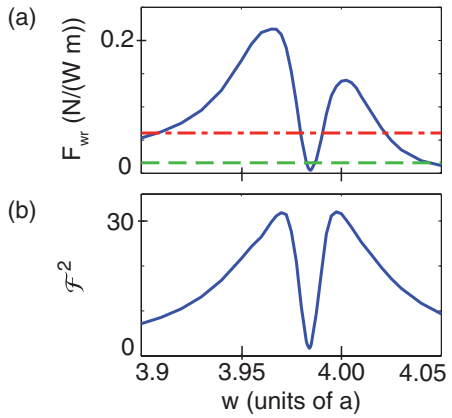

FIG. 4. (Color online) (a) F_{wr} for the two-resonator setup as a function of w, with the same parameters as in Fig. 3. The pressure for the two-waveguide-single-resonator setup (dashed) and the pressure for a one-waveguide-single-resonator system (dash-dotted), for the same L and d, are also shown for comparison. (b) $\mathcal{F}^2$ for the same setup as (a).

peaks in Fig. 3(c), and the magnitude of the pressure is an order of magnitude higher than the one-resonator case of Fig. 2(a). This indicates that the use of EIT provides a far superior mechanism for pressure enhancement as compared to the traditional single-resonator case. It is worth pointing out that at $w = 3.99a$, the system supports a dark resonance that does not show up as a transmission peak, since its external linewidth is narrower than its intrinsic linewidth, i.e., the system exhibits undercoupling. However, this dark resonance is excited, and therefore still results in a prominent peak in the pressure spectrum. Also, note that the peak positions of the pressure and transmission do not exactly line up, as is the nature of resonator optical pressure [13], and also because the transmission is the property of the two-resonator system, but the pressure is measured on the first resonator, which is an asymmetric measure and can create the shift.

By varying w and finding the maximum of the pressure spectrum, we plot in Fig. 4(a) the pressure as a function of w in comparison with the pressure from the one-resonator case [Fig. 1(b)] and the one-resonator–two-waveguide case [Fig. 1(d)]. In this EIT setup, the waveguide field in the section between the two resonators is enhanced by roughly the same ratio as the resonator field enhancement $\mathcal{F}$ [shown in Fig. 1(c)]; therefore, the maximum pressure occurs in this section, and the pressure enhancement factor is on the order of $\mathcal{F}^2$ due to the enhancement in both the cavity and the waveguide. We plot $\mathcal{F}^2$ in Fig. 4(b), and it is seen that the shapes and magnitude of the plot in Figs. 4(a) and 4(b) agree.

There are two interesting characteristics of the plot in Figs. 4(a) and 4(b). First, both graphs have two peaks with a dip at $w = w_0 = 3.985a$. Second, the field-enhancement [Fig. 4(b)] is symmetric around the dip, but the pressure [Fig. 4(a)] is slightly asymmetric. The cause of the asymmetry in the pressure graph comes from the choice of measuring the pressure only on the first resonator in this two-resonator system.

We now comment on the origin of the dip in Figs. 4(a) and 4(b). In the two-ring structure exhibiting the EIT effect, the external linewidth of the transparency resonance is at minimum when the cavity-cavity spacing w is chosen such that the EIT condition (destructive interference at the output) is satisfied at the frequency where T and R of the individual resonators are at the extremum [$f = 0.642c/a$, as seen in Fig. 3(b)]. This corresponds to $w = w_0 = 3.985a$ in our structure. Thus, as we vary the cavity-cavity spacing w toward w_0, we will initially see an enhancement in the pressure as the external quality factor increases. As we approach w_0, however, the transparency resonance eventually reaches the undercoupled regime with its external linewidth falling below its intrinsic linewidth, and hence the maximum pressure and field enhancement exhibits a dip in the immediate vicinity of $w \approx w_0$. Right at $w = w_0$, the pressure and the transmission peaks are very low, and would appear to be approximately zero if plotted in Figs. 3(c) and 3(d). As a function of w, the maximum pressure therefore should exhibit a peak in a relatively broad region of w around $w = w_0$, with a dip in the immediate vicinity of $w = w_0$, which is observed in Fig. 4(a).

As a final remark, we note that in the single-resonator case, reducing the intrinsic loss of the resonator does not enhance the waveguide-resonator force. On the other hand, in the EIT case, the force can be greatly enhanced if one were to reduce the intrinsic loss of the resonators, since in such a case the external linewidth of the transparency resonance can be further reduced without reaching the undercoupled regime. In conclusion, we have shown that the all-optical EIT analog provides a mechanism for enhancing optical forces, which may be important for optomechanical switching and frequency tuning.

This work is supported by an AFOSR-MURI program on Integrated Hybrid Nanophotonic Circuits (Grant No. FA9550-12-1-0024).

[1] K.-J. Boller, A. Imamoglu, and S. E. Harris, Phys. Rev. Lett. **66**, 2593 (1991).
[2] L. Maleki, A. B. Matsko, A. A. Savchenkov, and V. S. Ilchenko, Opt. Lett. **29**, 626 (2004).
[3] Q. Xu, S. Sandhu, M. L. Povinelli, J. Shakya, S. Fan, and M. Lipson, Phys. Rev. Lett. **96**, 123901 (2006).
[4] X. Yang, M. Yu, D. L. Kwong, and C. W. Wong, Phys. Rev. Lett. **102**, 173902 (2009).
[5] J. Pan, Y. Huo, S. Sandhu, N. Stuhrmann, M. L. Povinelli, J. S. Harris, M. M. Fejer, and S. Fan, Appl. Phys. Lett. **97**, 101102 (2010).
[6] Y. Huo, S. Sandhu, J. Pan, N. Stuhrmann, M. L. Povinelli, J. M. Kahn, J. S. Harris, M. M. Fejer, and S. Fan, Opt. Lett. **36**, 1482 (2011).
[7] D. D. Smith, H. Chang, K. A. Fuller, A. T. Rosenberger, and R. W. Boyd, Phys. Rev. A **69**, 063804 (2004).

[8] J. B. Khurgin, J. Opt. Soc. Am. B **22**, 1062 (2005).
[9] M. F. Yanik, W. Suh, Z. Wang, and S. Fan, Phys. Rev. Lett. **93**, 233903 (2004).
[10] N. Liu, T. Weiss, M. Mesch, L. Langguth, U. Eigenthaler, M. Hirscher, C. Sonnichsen, and H. Giessen, Nano Lett. **10**, 1103 (2010).
[11] B. Lukyanchuk, N. I. Zheludev, S. A. Maier, N. J. Halas, P. Nordlander, H. Giessen, and C. T. Chong, Nat. Mater. **9**, 707 (2010).
[12] C. M. Soukoulis and M. Wegener, Nat. Photon. **5**, 523 (2011).
[13] M. Li, W. H. P. Pernice, and H. X. Tang, Phys. Rev. Lett. **103**, 223901 (2009).
[14] M. Eichenfield, C. P. Michael, R. Perahia, and O. Painter, Nat. Photon. **1**, 416 (2007).
[15] A. Einat and U. Levy, Opt. Exp. **19**, 20405 (2011).
[16] G. S. Wiederhecker, L. Chen, A. Gondarenk, and M. Lipson, Nature (London) **462**, 633 (2009).
[17] G. S. Wiederhecker, S. Manipatruni, S. Lee, and M. Lipson, Opt. Exp. **19**, 2782 (2011).
[18] M. L. Povinelli, S. G. Johnson, M. Loncar, M. Ibanescu, E. J. Smythe, F. Capasso, and J. D. Joannopoulos, Opt. Exp. **13**, 8286 (2005).
[19] J. Rosenberg, Q. Lin, and O. Painter, Nat. Photon. **3**, 478 (2009).
[20] P. T. Rakich, M. A. Popovic, M. Soljacic, and E. P. Ippen, Nat. Photon. **1**, 658 (2007).
[21] P. T. Rakich, M. A. Popovic, and Z. Wang, Opt. Exp. **17**, 18116 (2009).
[22] M. L. Povinelli, M. Loncar, M. Ibanescu, E. J. Smythe, S. G. Johnson, F. Capasso, and J. D. Joannopoulos, Opt. Lett. **30**, 3042 (2005).
[23] www.comsol.com.
[24] M. Li, W. H. P. Pernice, and H. X. Tang, Nat. Photon. **3**, 464 (2009).
[25] H. A. Haus, *Waves and Fields in Optoelectronics* (Prentice-Hall, Englewood Cliffs, NJ, 1984).